Rock and Soil Mechanics

Volume 44 | Issue 11 Article 4

2-2-2024

Law of disturbed stress rotation induced by hard rock excavation and its influence on rock fracture

Qian-cheng SUN
National Field Observation and Research Station of Landslides in Three Gorges Reservoir Area of Yangtze River, China Three Gorges University, Yichang, Hubei 443002, China

Yue LIU
National Field Observation and Research Station of Landslides in Three Gorges Reservoir Area of Yangtze River, China Three Gorges University, Yichang, Hubei 443002, China

Qing-wen WANG
National Field Observation and Research Station of Landslides in Three Gorges Reservoir Area of Yangtze River, China Three Gorges University, Yichang, Hubei 443002, China

Shao-jun LI
State Key Laboratory of Geomechanics and Geotechnical Engineering, Institute of Rock and Soil Mechanics, Chinese Academy of Sciences, Wuhan, Hubei 430071, China

See next page for additional authors

Recommended Citation

SUN, Qian-cheng; LIU, Yue; WANG, Qing-wen; LI, Shao-jun; and ZHENG, Min-zong (2024) "Law of disturbed stress rotation induced by hard rock excavation and its influence on rock fracture," *Rock and Soil Mechanics*: Vol. 44: Iss. 11, Article 4.
DOI: 10.16285/j.rsm.2022.6726
Available at: https://rocksoilmech.researchcommons.org/journal/vol44/iss11/4

Law of disturbed stress rotation induced by hard rock excavation and its influence on rock fracture

Abstract

The rock fracture caused by disturbed stress field change in deep underground engineering is a common issue receiving continuous attention. After analyzing the test data of disturbed stress field in Jinping underground laboratory phase II project, the variation law of disturbed stress field under different construction processes was interpreted, and the change mode of principal stress direction was analyzed. Through the comparative analysis about in-situ drilling imaging of rock mass, the influence of principal stress direction change on surrounding rock fracture was revealed. The results show that the disturbed stress field changes the most actively at the stage of middle pilot tunnel excavation, the change mode of principal stress direction is mainly gyration when the tunnel face is advancing toward the monitoring section, and the change mode is mainly rotation when the tunnel face moves away from the monitoring section. The position where the principal stress direction change reaches the maximum is 4.5 meters away from the design profile of test tunnel. During the expanded excavation of sidewall, the change mode of principal stress direction is mainly rotation, and the position where the change reaches the maximum is 2.5 meters away from the design profile of test tunnel. The change in disturbed stress direction directly affects the pattern and trend of rock fracture development, the stress with large-angle rotation tends to cause tensile crack and tensile-shear mixed crack, and the stress with small-angle rotation tends to cause the shear crack with concave and convex morphological features whose deflection angle equals the stress rotation angle. The stress with large-angle gyration mostly causes X-shaped shear crack. The results based on the measured disturbed stress can provide a reference for studying the variation law of disturbed stress field during deep high-stress hard rock excavation and its influence on rock facture development.

Keywords

deep rock mass, hard rock excavation, disturbed stress, stress direction, rock facture

Authors

Qian-cheng SUN, Yue LIU, Qing-wen WANG, Shao-jun LI, and Min-zong ZHENG

Rock and Soil Mechanics 2023 44(11): 3128−3140 ISSN 1000−7598
https://doi.org/10.16285/j.rsm.2022.6726 https://rocksoilmech.researchcommons.org/journal/

Law of disturbed stress rotation induced by hard rock excavation and its influence on rock fracture

SUN Qian-cheng[1], LIU Yue[1], WANG Qing-wen[1], LI Shao-jun[2], ZHENG Min-zong[2]

1. National Field Observation and Research Station of Landslides in Three Gorges Reservoir Area of Yangtze River, China Three Gorges University, Yichang, Hubei 443002, China

2. State Key Laboratory of Geomechanics and Geotechnical Engineering, Institute of Rock and Soil Mechanics, Chinese Academy of Sciences, Wuhan, Hubei 430071, China

Abstract: The rock fracture caused by disturbed stress field change in deep underground engineering is a common issue receiving continuous attention. After analyzing the test data of disturbed stress field in Jinping underground laboratory phase II project, the variation law of disturbed stress field under different construction processes was interpreted, and the change mode of principal stress direction was analyzed. Through the comparative analysis about in-situ drilling imaging of rock mass, the influence of principal stress direction change on surrounding rock fracture was revealed. The results show that the disturbed stress field changes the most actively at the stage of middle pilot tunnel excavation, the change mode of principal stress direction is mainly gyration when the tunnel face is advancing toward the monitoring section, and the change mode is mainly rotation when the tunnel face moves away from the monitoring section. The position where the principal stress direction change reaches the maximum is 4.5 meters away from the design profile of test tunnel. During the expanded excavation of sidewall, the change mode of principal stress direction is mainly rotation, and the position where the change reaches the maximum is 2.5 meters away from the design profile of test tunnel. The change in disturbed stress direction directly affects the pattern and trend of rock fracture development, the stress with large-angle rotation tends to cause tensile crack and tensile-shear mixed crack, and the stress with small-angle rotation tends to cause the shear crack with concave and convex morphological features whose deflection angle equals the stress rotation angle. The stress with large-angle gyration mostly causes X-shaped shear crack. The results based on the measured disturbed stress can provide a reference for studying the variation law of disturbed stress field during deep high-stress hard rock excavation and its influence on rock facture development.

Keywords: deep rock mass; hard rock excavation; disturbed stress; stress direction; rock facture

1 Introduction

In deep engineering, the rock masses disturbed by excavation usually undergo complex stress adjustment such as tangential loading, radial unloading, and principal stress direction change[1], and the redistribution of the secondary stress in surrounding rock is then caused, which leads to the initiation and expansion of cracks in the rock masses. Zheng et al.[2] derived the theoretical formula of plastic deformation increment caused by rotational stress component based on generalized plastic mechanics. In fact, both the magnitude and direction of stress in surrounding rock may change under the excavation disturbance. It is a common understanding that the stress field change in surrounding rock due to excavation affects the surrounding rock stability.

The relationships between stress state and rock damage or fracture were explored by means of laboratory triaxial test, true triaxial test, torsional-shear test, acoustic emission monitoring, and numerical simulation. Sha et al.[3] studied the unloading strength and fracture evolution characteristics of Jinping marble under different stress paths and loading rates by true triaxial unloading tests, and revealed that the unloading failure of marble followed the processes of tensile initiation–shear intersection–coalescence failure. Through true triaxial tests, Liu et al.[4] concluded that the failure mode of granite under loading and unloading was tensile-shear mixed failure, and the macroscopic crack propagation direction was closely related to the principal stress direction. Wang et al.[5] analyzed the propagating mechanism of top-coal fracture in longwall top-coal caving mining by laboratory test and numerical simulation, and found that the principal stress direction rotation would lead to the inclination of top-coal fracture to the goaf. Gao et al.[6] examined the types and mechanisms of stress-induced spalling of deep hard rock through laboratory test and numerical simulation. Pang et al.[7] investigated the change laws of mining-induced stress during rock fracture by numerical simulation, and found that the damage and separation of overlying strata were mainly affected by the state and transformation form of three-dimensional mining-induced stress. Zhong et al.[8] examined the strength and deformation characteristics of calcareous sand under different stress paths through laboratory tests. Based on the numerical simulation results, Zhang et al.[9] deemed that the fracture depth was controlled by the change of stress magnitude, and the fracture

Received: 3 November 2022 Accepted: 3 January 2023
This work was supported by the National Natural Science Foundation of China (51909136, 42202320).
First author: SUN Qian-cheng, female, born in 1988, PhD, Associate Professor, mainly engaged in teaching and research related to geotechnical engineering. E-mail: qc_sun@ctgu.edu.cn;
Corresponding: LI Shao-jun, male, born in 1974, PhD, Professor, mainly engaged in research on deep rock mechanics and engineering safety. E-mail: sjli@whrsm.ac.cn

density was controlled by the change of stress direction. Sun et al.[10] believed that the essence of principal stress rotation was that there was a shear component in stress increment, and the stress rotation during tunnel excavation would cause a sudden increase in the plastic deformation of cracks. Zhang et al.[11] explored the influence mechanism of intermediate principal stress, stress path, and rotation of principal stress axis on rock crack propagation. Building on numerical simulation, Li et al.[12] revealed the key role of stress principal axis rotation in meso-crack propagation, surrounding rock damage, and rock strength degradation. Chang et al.[13] found that the crack propagation direction would shift during principal stress rotation.

In addition, the investigation of influence of stress field changes in rock masses on surrounding rock fracture was also carried out. Kaiser et al.[14] believed that stress rotation would disturb the pre-existing discontinuities under shear stress, resulting in crack propagation, joint opening, or rock bridge break. Eberhard[15] explored the near-field stress path change when tunnel face was advancing, and concluded that the rotation of principal stress axis controlled the rock fracture propagation direction. Diederichs et al.[16] showed that the damage caused by stress rotation would reduce the crack interaction threshold near the excavation section. Shalev et al.[17] demonstrated that the propagation direction of rock fracture was closely related to the principal stress direction.

The existing research results showed the changes of deformation process, rock strength, and fracture mode when the stress state in laboratory rock changes, and discussed the influence of rock stress rotation on the plastic deformation development, crack propagation process, failure mode change, and engineering stability state of surrounding rock under different working conditions, which provides an important theoretical basis for the study of rock fracture induced by stress adjustment under unloading conditions. However, the actual occurrence environment of engineering rock mass is complex, and there exist many factors affecting the development of rock damage or fracture, so it is difficult to accurately consider the spatotemporal effects of stress adjustment in laboratory tests and numerical simulations.

Based on the measured data of disturbed stress during excavation in Jinping deep underground laboratory, the spatial distribution characteristics of disturbed stress were analyzed, the correlations between disturbed stress and rock damage or fracture during different construction processes were discussed, and the influence of disturbed stress field direction change on rock fracture mode was further explored.

2 Project overview

2.1 Engineering background

The Jinping deep underground laboratory phase II project is located in Jinping Mountain at the junction of Muli, Yanyuan, and Mianning counties in Liangshan Yi Autonomous Prefecture, Sichuan Province. The buried depth of the laboratory is about 2 400 m, and the laboratory belongs to the ultra-deep underground laboratory. The main body of the underground laboratory is composed of four scattered test tunnels, whose length is 130 m. There are two physics laboratories with a length of 65 m in each test tunnel, and they are A1, A2, B1, B2, C1, C2, D1, and D2 laboratories from west to east. B3 and B4 laboratories are set beside B1 and B2 laboratories as deep rock mechanics laboratories with a length of 60 m (30 m in both eastern and western directions), forming a pattern of 4 tunnels and 9 laboratories in general. The axial directions of the test tunnels are all parallel to those of Jinping auxiliary tunnel, and the azimuth angle of the axis is N58°W. The project site is located in the anticline region with the strike of N27°E, and the location of the traffic tunnel axis is the anticline core. Two faults are developed in the project site, which extend for a long distance and are staggered anticline structures, with a maximum width of about 1 m[18–20]. The layout of the project site is shown in Fig. 1.

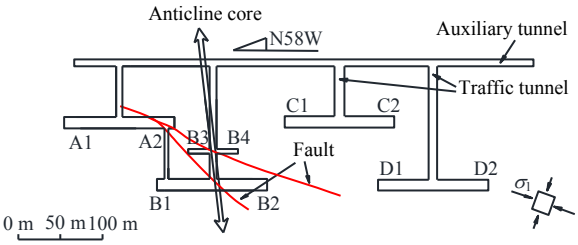

Fig. 1 Plane layout of underground chamber

The main test tunnels are all in city wall gate shape with excavation section of 14 m×14 m, which were excavated by drilling and blasting, and had gone through four construction stages: upper middle drift excavation (I), expanded excavation of side wall (II), middle layer excavation (III), and lower layer excavation (IV).

2.2 Monitoring overview

For the disturbed stress testing in B2 laboratory during excavation, the boreholes were preset in the direction from B4 laboratory to B2 laboratory, and six groups of three-dimensional disturbed stress testing devices at various distances from the designed side wall of laboratory were embedded. The distances between each group of testing devices and the design profile of test tunnel were 2.5 m, 4.5 m, 6.5 m, 8.5 m, 12.5 m, and 16.5 m, respectively, and the layout is shown in Fig. 2. At the same time, parallel boreholes were set to carry out long-term in-situ borehole testing to obtain the damage and fracture characteristics of rock mass during excavation.

The disturbed stress testing system was a self-developed single-hole multi-point fiber Bragg grating (FBG) hollow inclusion three-dimensional stress testing device[21]. The device consists of several unit FBG cylindrical hollow inclusion stress gauges, rigid connecting rod, centering bracket, wavelength demodulator, and computer. The unit FBG cylindrical hollow

inclusion stress gauges are composed of epoxy resin hollow inclusion, rigid connecting end ring, and optical fiber, as shown in Fig. 3. The pressure grouting was used to backfill the borehole at the set position where the sensor was buried, and the grouting pressure and filling amount were controlled. After the grouting strength was reached, the trial collection started. The necessary temperature and stress compensations were performed according to the previous testing data, and the initial test parameters were set. The data collected before laboratory excavation was stable, which showed that the testing system was effective.

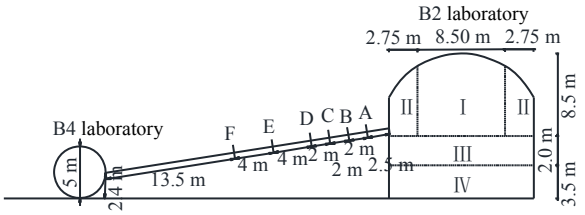

Fiber bragg grating stress sensor layout at K0+030 section in B2 laboratory

Fig. 2 Layout of disturbed stress monitoring points in B2 laboratory

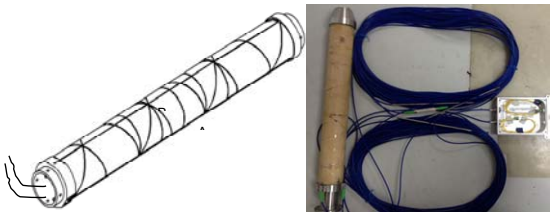

Fig. 3 Three-dimensional disturbed stress testing sensor

3 Change laws of principal stress direction

Three principal stresses ($\sigma_1, \sigma_2, \sigma_3$) at point *O* in space are projected onto the *XOY* plane to get the stress vector projection. However, the dip angle change in the projection cannot be clearly expressed because of the nonlinearity of different dip angle projection onto the *XOY* plane.

To distinguish the change degree of the dip angle on the vector diagram and make the stress rotation degree more clearly shown in the diagram, the stress azimuth angle is obtained by clockwise rotation from the due north direction (set as *y* axis) in the stress azimuth diagram, and the dip angle is the distance from the circle center to the point. The point is on the circle center when the dip angle is 90° , the point is on the arc when the dip angle is 0° , and the intermediate angle is obtained by linear interpolation.

The in-situ stress testing results obtained at this project site based on the principle of strain relief[22] are shown in Fig. 4(b). The values marked in the brackets at a single point in Fig. 4(b) are the azimuth angle, dip angle, and stress value.

The azimuth angle of the maximum principal stress is 326.04 °, the dip angle is 55.60 °, and the stress value is 69.20 MPa, which is close to the estimated self-weight of overlying strata. The two principal stresses near the horizontal plane are the minimum principal stress and the intermediate principal stress. The azimuth angle of the minimum principal stress is 70.90 °, the dip angle is 9.98 °, and the stress value is 25.54 MPa. Based on the in-situ stress field, the distribution of disturbed stress field can be obtained by superimposing the disturbed stress testing data. The changes of the same stress component at a point on multiple time scales are depicted on the stress vector diagram, and connected by smooth curves in time sequence, so as to obtain the change path of the stress at this point, as shown in Fig. 4 (c).

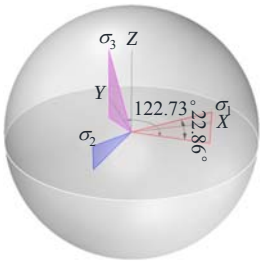

(a) Vector projection of stress in three directions at a point in space

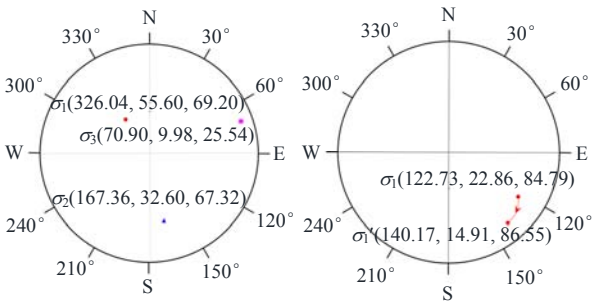

(b) Stress vector diagram at a single point

(c) Schematic diagram of stress changes

Fig. 4 Spatial projection of stress vector

The stress testing results during the whole excavation process show that the changes of disturbed stress direction are the most active at the stages of the middle pilot tunnel excavation. The testing results of each monitoring point were analyzed when the tunnel face and the monitoring section are in different position relations (Fig.5 shows the position relations between the monitoring section and the tunnel face at the stage of the middle pilot tunnel excavation), and the stress changes at different monitoring points in different excavation stages were explained.

3.1 Principal stress rotation induced by middle pilot tunnel excavation

The results at the monitoring point 2.5 m away from the design profile of test tunnel show that the gyration of the three principal stresses all occur when the tunnel face advances from the position of −10–0 m away from the monitoring section. The three principal stresses all rotate in different degrees from the initial angle, and finally return to the position not far away

from the initial angle. The azimuth angle range of the maximum principal stress is around 105°–135°, and the dip angle is about 20°. The azimuth angle of intermediate principal stress ranges from −15° to 30°, and the dip angle is about 50°. The azimuth angle range of minimum principal stress is around 20°–60°, and the dip angle is about 30°, as shown in Fig. 6 (a). During the advancing process of the tunnel face, the maximum rotation angle of the three principal stresses is nearly 90°, the azimuth angle of the maximum principal stress rotates from 130° to about 220°, and the dip angle changes between 5° and 22°. The azimuth angle of the intermediate principal stress rotates from 30° to −40°, and the dip angle increases first and then decreases during rotation, with the maximum rotation reaching 50° and the minimum rotation reaching nearly 20°. The minimum principal stress azimuth is rotated from 40° to 90°, and the dip angle is increased from 30° to 60°, as shown in Fig. 6 (b). After the tunnel face passes beyond 10 m through the monitoring section, the excavation has little influence on the principal stress angle at the monitoring point, and the maximum rotation angles of the three principal stresses are below 2°, as shown in Fig. 6 (c).

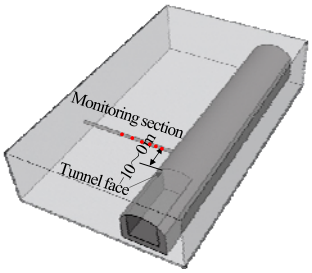

(a) –10～0 m before reaching the monitoring section

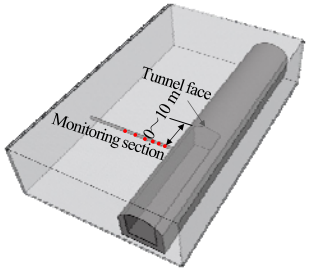

(b) 0～10 m crossing the monitoring section

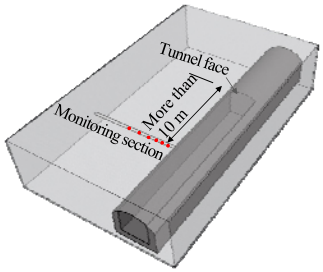

(c) More than 10 m crossing the monitoring section

Fig. 5 Typical positions of tunnel face away from monitoring section during middle pilot tunnel excavation

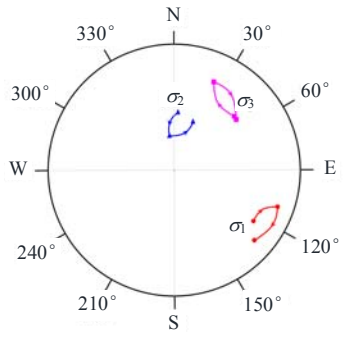

(a) –10 m to 0 m away from the monitoring section

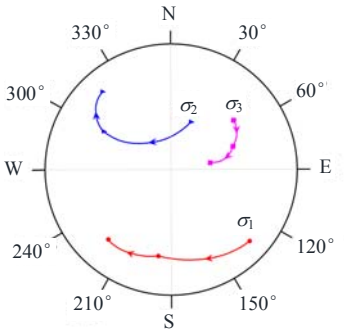

(b) Passes 0 m to 10 m away from the monitoring section

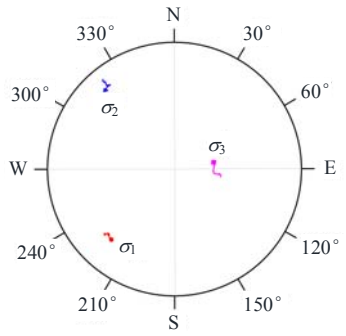

(c) Passes beyond 10 m away from the monitoring section

Fig. 6 Results at monitoring points 2.5 m away from design profile of test tunnel during middle pilot tunnel excavation

The results at the monitoring point 4.5 m away from the design profile of test tunnel show that the gyration of the three principal stresses all occur when the tunnel face advances towards the monitoring section. The azimuth angle range of the maximum principal stress is about 65°, and the dip angle decreases from 31° to 16° and then turns back to 30°, showing a process of first decreasing and then increasing. The azimuth angle of the intermediate principal stress ranges from 150° to 180°, the dip angle increases first and then decreases, rotates from 21° to 42° and then turns back to 22°. The azimuth angle range of the minimum principal stress is around 280°–310°, and the dip angle rotates from 55° to 35° and then back to 54°, showing a process of first decreasing and then increasing, as shown in Fig.7 (a). The direction of stress rotation is more evident when the tunnel face continues to advance about 10 m from the monitoring section, and the maximum single rotation angle is about 90°. The azimuth angle of the

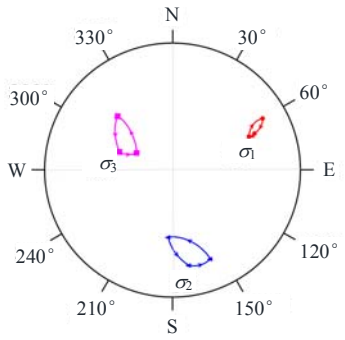

(a) –10 m to 0 m away from the monitoring section

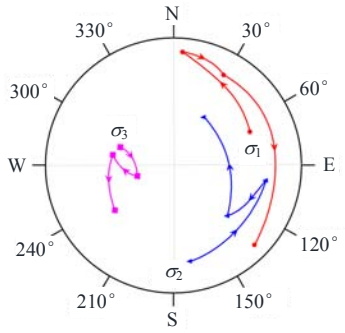

(b) Passes 0 m to 10 m away from the monitoring section

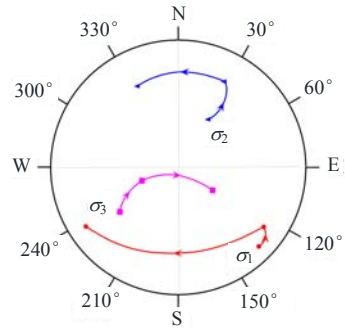

(c) Passes beyond 10 m away from the monitoring section

Fig. 7 Results at monitoring points 4.5 m away from design profile of test tunnel during middle pilot tunnel excavation

maximum principal stress first rotates to near the north direction, then rotates to around 30°, and then rotates nearly 90° to about 135°, and the dip angle decreases from 25° to 10°. The azimuth angle of the intermediate principal stress first rotates to near the east and then rotates back to about 125°, then rotates nearly 90° to about 30°, and the dip angle increases from 23° to 50°. The azimuth angle of the minimum principal stress decreases from 293° to 232°, and the dip angle gradually decreases to 40° after a small rotation, as shown in Fig.7 (b). When the tunnel face is more than 10 m away from the monitoring section, the stress rotation angle is large, and the maximum rotation angle of the three principal stresses is nearly 100°. The azimuth angle of the maximum principal stress rotates from 132° to 235°, and the dip angle increases from 11° to 16°. The azimuth angle of the intermediate principal stress rotates from 35° to 330°, and the dip angle decreases from 31° to 21°. The minimum principal stress azimuth is rotated from 240° to 112°, and the dip angle is increased from 56° to 64°, as shown in Fig.7(c). Compared with the first two monitoring points, when the tunnel face is away from the monitoring section at different distances, the rotations of the three principal stresses at the monitoring point 6.5 m away from the side wall are significantly reduced to about 20°, and the stresses rotate in small ranges, as shown in Figs.8(a)–8(c). As shown in the pictures, the azimuth angle of the maximum principal stress basically changes around 210°–230°, and the dip angle is close to horizontal (close to circular arc). The azimuth angle of the intermediate principal stress also changes around 30°–70°, and the dip angle changes near the vertical direction (near the circle center). The azimuth angle of the minimum principal stress varies from 125° to 135°, and the dip angle is nearly horizontal. When the distance between the tunnel face and the monitoring section is different, the three principal stress directions at this point are adjusted slightly, and the excavation activity at different sections has a minimal effect on the stress rotation of surrounding rock at a depth of 6.5 m in the radial direction of the tunnel.

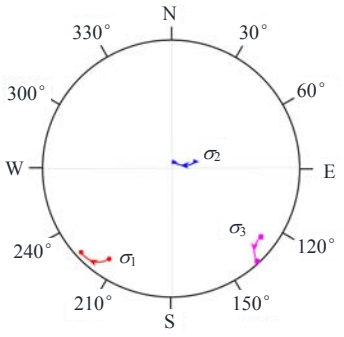

(a) –10 m to 0 m away from the monitoring section

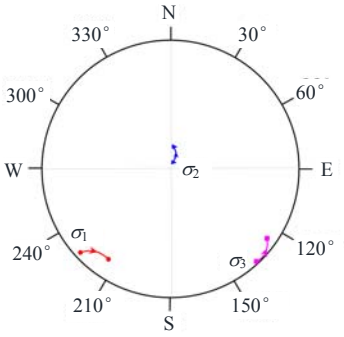

(b) Passes 0 m to 10 m away from the monitoring section

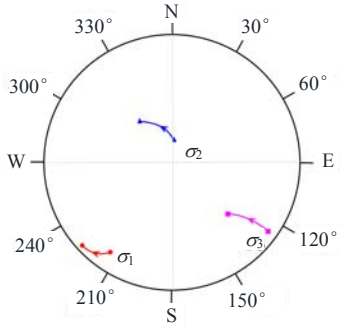

(c) Passes beyond 10 m away from the monitoring section

Fig. 8 Results at monitoring points 6.5 m away from design profile of test tunnel during middle pilot tunnel excavation

In the three advancing stages of tunnel face, the rotation ranges of three principal stress directions at the monitoring point 8.5 m away from the side wall are very small, and the maximum rotation angle is about 10°, which occurs at the stage when the tunnel face just passes through the monitoring section. The angle changes of the principal stress at this point and the monitoring point at 6.5 m are not large, and the three principal stresses only rotate to a certain extent after the tunnel face passes through the monitoring section, as shown in Figs. 9(a)–9(c).

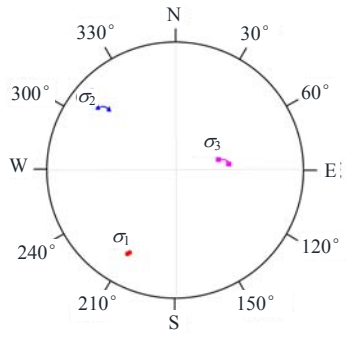

(a) –10 m to 0 m away from the monitoring section

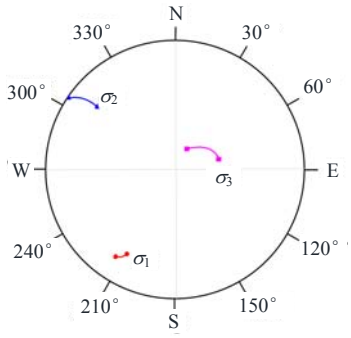

(b) Passes 0 m to 10 m away from the monitoring section

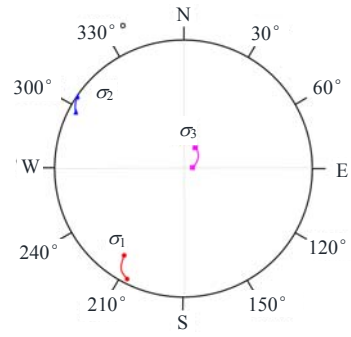

(c) Passes beyond 10 m away from the monitoring section

Fig. 9 Results at monitoring points 8.5 m away from design profile of test tunnel during middle pilot tunnel excavation

During pilot tunnel excavation, the stress direction at each monitoring point changes. When the distance from the side wall is 6.5–8.5 m, the three principal stresses in surrounding rock only change in a very small range. The influence of excavation disturbance on the monitoring points at different distances from the side wall differs, and the change of principal stress direction is also different. The closer to the side wall, the greater the influence of excavation disturbance, and the greater the stress rotation. At the stage of middle pilot tunnel excavation, the maximum change of the principal stress direction occurs at the monitoring point 4.5 m away from the side wall.

3.2 Principal stress rotation induced by expanded excavation of side wall

The results at the monitoring point 2.5 m away from the design profile of test tunnel show that the change of principal stress angle is small when the excavation face advances to the monitoring section, and the azimuth angle of the maximum principal stress is around 235°, and the dip angle is about 16°. The azimuth angle of the intermediate principal stress is around 325°, and the dip angle is about 7°. The azimuth angle of the minimum principal stress is about 35°, and the dip angle is about 70°, as depicted in Fig.10(a). When the excavation face continues to advance from the monitoring section, the azimuth angle of the maximum principal stress rotates from 238° to 220°, and the dip angle is about 20°. The azimuth angle of the intermediate principal stress rotates from 325° to 310°, and the dip angle is about 5°. The azimuth angle of the minimum principal stress rotates from 23° to 36°, and the dip angle is about 70°, with small change, as presented in Fig.10(b). Once the excavation face is 10 meters away from the monitoring section, there is a significant cyclic rotation in the directions of the three principal stresses at this measuring point, and the rotation of the stress azimuth angle approaches 90 ° several times. The azimuth angle of the maximum principal stress first rotates from 200° to 145°, the dip angle increases from 21° to 50°. Then the azimuth angle rotates from 145° to 45°, and the dip angle increases from 50° to 70°. After a period of time, the directions recover to the stress directions before rotation. The stress undergoes two jumps, and finally rotates to the state with an azimuth angle of nearly 90° and a dip angle of about 50°, which deviates 20° from the cyclic jumping direction of stress. The azimuth angle of the intermediate principal stress first rotates from −50° to 40°, and the dip angle increases from near horizontal direction to about 15°. Then the azimuth angle rotates from 40° to −60°, and the dip angle decreases from 15° to 10°. After a period of time, the directions return to the stress directions before rotation. The stress goes through two cyclic jumps, and finally rotates to the state with an azimuth angle of nearly 10° and a dip angle of about 10°, which deviates 20° from the cyclic jumping direction of stress. The azimuth angle of the minimum principal stress first rotates from 40° to −60°, and the dip angle decreases from 68° to 36°. Then the azimuth angle rotates from −60° to −146°, and the dip angle decreases from 36° to 15°. After a period of time, the directions return to the stress directions before rotation. The stress undergoes two cyclic jumps, and finally rotates to the state with an azimuth angle of −60° and a dip angle of about 37°,

which is the direction before stress jump, as displayed in Fig.10(c). At this stage, the gyration of the three principal stresses appears, the stress directions return to the directions before rotation after two rotations of nearly 90°. The complete duration of a single stress gyration is about 3−5 days, and the time interval between the two stress rotations is about 20 days.

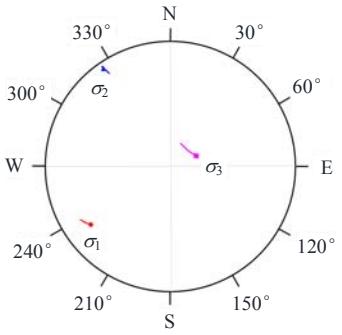

(a) –10 m to 0 m away from the monitoring section

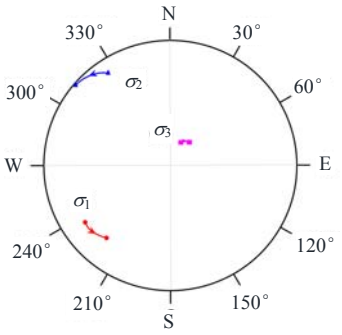

(b) Passes 0 m to 10 m away from the monitoring section

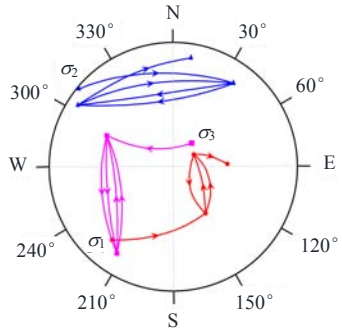

(c) Passes beyond 10 m away from the monitoring section

Fig. 10 Results at monitoring points 2.5 m away from design profile of test tunnel during expanded excavation of side wall

As the excavation face advances towards the monitoring section, the maximum rotation angle of the principal stress at the monitoring point 4.5 m away from the side wall is nearly 45°. The azimuth angle of the maximum principal stress is about 240°, and the dip angle is close to the horizontal direction. The azimuth angle of the intermediate principal stress rotates from −30° to near due north, and the dip angle increases from 25° to 70°. The azimuth angle of the minimum principal stress is rotated from 120° to 150°, and the dip angle is reduced from 62° to 19°, as given in Fig.11(a). When the excavation face continues to advance from the monitoring section for about 10 m, the angle of the maximum principal stress hardly changes, while the angles of the intermediate principal stress and the minimum principal stress change, and the maximum rotation angle is about 15°, as shown in Fig.11(b). When the excavation face exceeds the monitoring section by 10 m, the directions of the three principal stresses almost no longer change, as shown in Fig. 11(c).

The results at the monitoring point 6.5 m away from the side wall show that the rotation angles of the three principal stresses are very small when the excavation face approaches the monitoring section, and the maximum rotation angle is about 5°. The continuous advancement of the excavation face through the monitoring section has almost no influence on the stress disturbance in surrounding rock, and no conspicuous rotation in the three principal stresses have been observed, as shown in Figs.12(a) and 12(b).

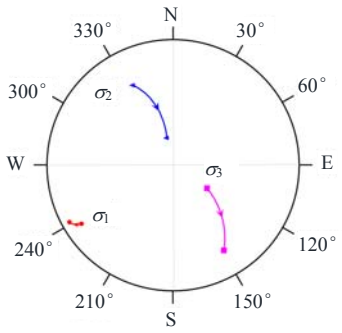

(a) –10 m to 0 m away from the monitoring section

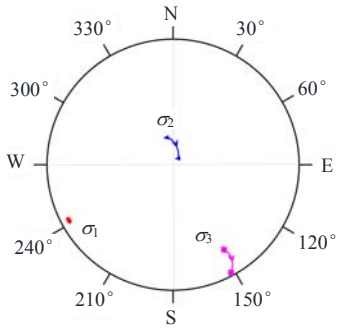

(b) Passes 0 m to 10 m away from the monitoring section

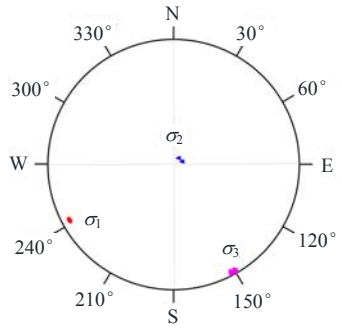

(c) Passes beyond 10 m away from the monitoring section

Fig. 11 Results at monitoring points 4.5 m away from design profile of test tunnel during expanded excavation of side wall

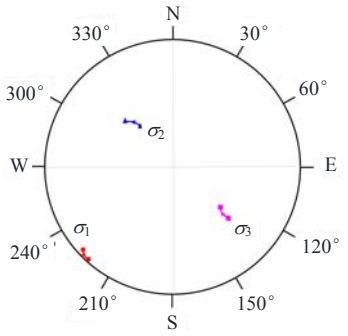

(a) –10 m to 0 m away from the monitoring section

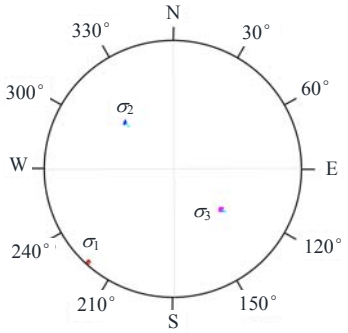

(b) Passes 0 m to 10 m away from the monitoring section

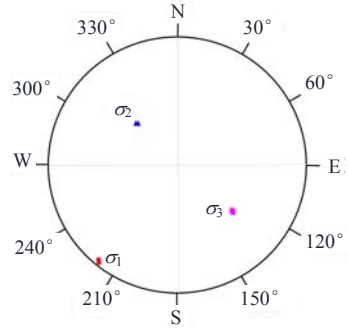

(c) Passes beyond 10 m away from the monitoring section

Fig. 12 Results at monitoring points 6.5 m away from design profile of test tunnel during expanded excavation of side wall

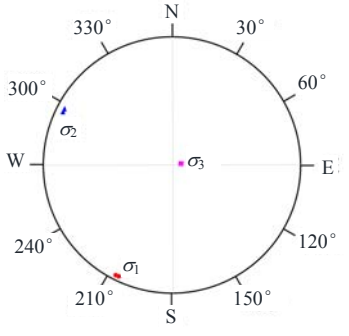

(a) –10 m to 0 m away from the monitoring section

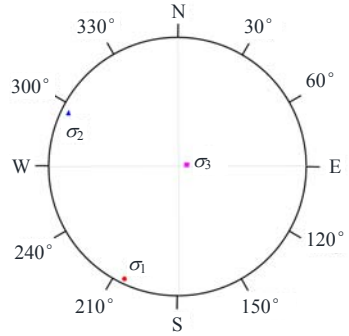

(b) Passes 0 m to 10 m away from the monitoring section

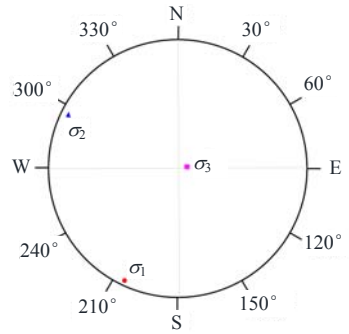

(c) Passes beyond 10 m away from the monitoring section

Fig. 13 Results at monitoring points 6.5 m away from design profile of test tunnel during expanded excavation of side wall

The results at the monitoring points at 8.5 m away from the side wall show that the directions of the three principal stresses no longer change when the excavation face advances during the expanded excavation of the side wall, and the influence of side wall excavation on the stress direction rotation disappears completely at this point, as shown in Figs. 13(a)–13(c).

Compared with the stage of middle pilot tunnel excavation, the stress direction changes at the monitoring points at different distances from the side wall are reduced during the expanded excavation of the side wall, and the sudden change of stress direction is caused only in the construction process after the excavation face passes 10 m over the monitoring section, especially the stress direction at the monitoring points 2.5 m away from the side wall has two cyclic rotations of nearly 90°. During expanded excavation of the side wall, the farther the point away from the side wall, the smaller the stress rotation.

3.3 Principal stress change mode in different construction processes

By analyzing the stress direction changes at each measuring point in different construction processes, the stress direction changes during the middle pilot tunnel excavation and expanded excavation of the side wall are summarized as shown in Table 1. The stress direction changes can be summarized into two types of modes, namely stress rotation and stress gyration.

(1) Stress rotation means that the stress direction deviates from the original position and deflects in favor of rock mass unloading, and the typical changes are shown in Figs. 6(b) and 7(b). Rotation of stress angle is the normal state of stress adjustment after disturbance on rock mass. The greater the disturbance on rock mass, the faster the rotation speed and the longer the influence period. For this rotation mode, the azimuth angle of the stress changes markedly, especially after the tunnel face passes through the monitoring section. When the complete rock mass near the monitoring

section is excavated to form a free surface, the stress direction is easier to change in the excavation direction (tunnel axial direction) and unloading direction (tunnel radial direction), that is, in the horizontal plane.

Table 1 Stress rotation modes at different monitoring points during different excavation processes

Process	Monitoring point /m	–10 m to 0 m away from the monitoring section	Passes 0 m to 10 m away from the monitoring section	Passes beyond 10 m away from the monitoring section
Middle drift excavation	2.5	Small gyration	Sudden rotation	Slow rotation
	4.5	Small gyration	Sudden rotation	Slow rotation+sudden rotation
	6.5	Slow rotation	Slow rotation	Slow rotation
	8.5	Slow rotation	Slow rotation	Slow rotation
Expanded excavation of side wall	2.5	Slow rotation	Slow rotation	Large gyration
	4.5	Sudden rotation	Slow rotation	Almost no rotation
	6.5	Slow rotation	Almost no rotation	Almost no rotation
	8.5	Almost no rotation	Almost no rotation	Almost no rotation

(2) Stress gyration refers to that the stress direction returns to or moves near the original stress direction after the stress direction changes. The gyration is a combination of multiple rotations, and typical changes are shown in Figs. 6(a) and 7(a). The gyration of stress angle occurs at the initial stage of stress adjustment in surrounding rock affected by excavation or after penetration of new cracks, and can be divided into small gyration and large jump gyration according to the magnitude of direction change. In the stress gyration mode, the azimuth angle and dip angle of stress generally change to a certain extent.

4 Influence of stress rotation on rock crack development

4.1 Theoretical analysis

In the rock fracture mechanics theory, the crack development in rock mass under compressive stress is usually simplified as a model where uniform uniaxial pressures σ_1 and σ_3 are loaded on the edge of infinite linear elastic plate and micro-cracks are replaced by flat elliptical holes, as shown in Fig. 14.

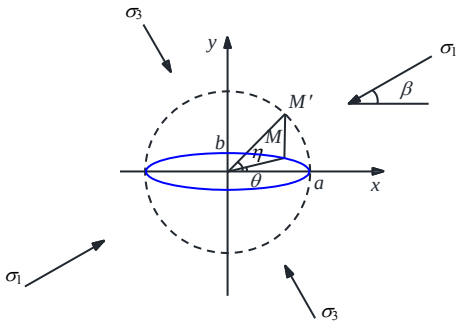

Fig. 14 Flat ellipse model for microcrack propagation in rock mass

According to the flat elliptical model in fracture mechanics[23], a quantitative expression of the circumferential stress distribution $\sigma_{\eta\eta}$ is

$$\sigma_{\eta\eta}=(\sigma_1+\sigma_3)\,\mathrm{sh}\,2\xi-(\sigma_1-\sigma_3)[\mathrm{e}^{2\xi}\cos(\beta-\eta)-\cos 2\beta]/(\mathrm{ch}\,2\xi-\cos 2\eta) \tag{1}$$

where β is the angle between the long axis direction of elliptical crack and the direction of σ_1, which is called crack angle; ξ and η are the elliptical coordinates of points on the plane, which corresponds to r and θ in polar coordinates; $\xi=\mathrm{arccha}\,c/c$, and $c=(a^2+b^2)^{\frac{1}{2}}$, where a and b are the major axes and minor axes of oblate elliptical cracks.

When the micro-crack is replaced by a flat elliptical hole and ξ is very small, $\xi\approx b/a$. The maximum and minimum values of the circumferential stress are obtained by differentiating Eq.(1) with η as an independent variable, and the condition for the maximum circumferential stress occurrence at the hole edge is

$$\eta=2\xi(\sigma_1\sin^2\beta+\sqrt{\sigma_1^2\sin^2\beta+\sigma_2^2\cos^2\beta}+\sigma_3\cos^2\beta)/(\sigma_1-\sigma_3)\sin 2\beta \tag{2}$$

By substituting Eq.(2) into Eq.(1), the maximum tensile stress $(\sigma_{\eta\eta})_{\max}$ assumed to cause failure on the inner surface of the notch is

$$(\sigma_{\eta\eta})_{\max}=\frac{1}{\xi}(\sigma_1\sin^2\beta+\sigma_3\cos^2\beta+\sqrt{\sigma_1^2\sin^2\beta+\sigma_3^2\cos^2\beta}) \tag{3}$$

According to Eq.(3), the actual crack propagation direction is not along the original direction under the stress rotation condition. When the stress is constant, the first-order differential of the crack angle β in Eq.(3) is 0, and the dominant crack propagation angle β_{m} corresponding to the maximum tensile stress at the hole edge can be obtained as

$$\beta_{\mathrm{m}}=\arccos\left(\frac{1}{2}\sqrt{\frac{3\sigma_1+\sigma_3}{\sigma_1+\sigma_3}}\right) \tag{4}$$

According to Griffith's fracture criterion, when the energy release rate equals the surface energy required for crack propagation, micro-cracks in rock mass begin to propagate. When the stress direction in rock mass rotates, the "relative initial angle" of crack angle changes, and the crack propagation direction breaks away from the original crack plane and expands towards the maximum principal stress direction after rotation, resulting in secondary wing cracks that make the crack break away from the original crack plane and develop into a crack with "protruding angle". Under the excavation disturbance, the stress in rock mass rotates many times, resulting in the development

of many new cracks with different directions from the original cracks, which is consistent with the results obtained by Eberhardt[15] using numerical simulation.

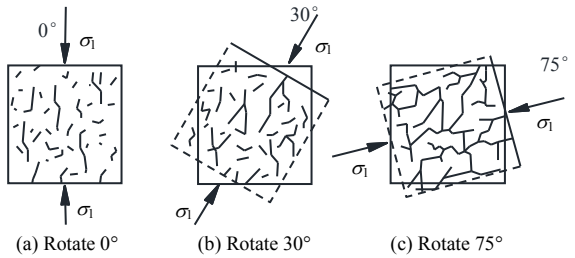

Fig. 15 Coalescence mechanism of rock mass under principal stress rotation

4.2 Rock fracture analysis based on borehole imaging

The in-site measured borehole imaging data are displayed in Fig. 16, in which black lines represent the cracks collected for the first time by preset boreholes, also the original cracks before tunnel excavation, red lines represent the new cracks initiated during excavation, and blue lines indicate that the original cracks are opened.

The imaging results of preset boreholes adjacent to stress measurement holes at different excavation stages are depicted in Fig.16. During middle pilot tunnel excavation, the three principal stresses rotate nearly 90° during the advancement of the tunnel face from 10 m away from the monitoring section to 10 m passing through the monitoring section, and the maximum principal stress rotates from along the tunnel axis to perpendicular to the tunnel axis, as shown in Figs. 6(a) and 6(b). Under the influence of stress rotation, two splitting tensile cracks ① and ② develop in the preset borehole at the position 0.2 m away from the design profile of test tunnels along the direction of maximum principal stress after rotation at a certain angle with the original cracks, as shown in Fig. 17. A tensile crack ③ develops at the position nearly 0.5 m away from the design profile of test tunnels, which deviates from the fracture direction under the influence of stress rotation, and presents a prominent folding angle of 90° in the borehole imaging map, forming a special crack shape in the form of "protruding angle". This kind of fracture is caused by the sudden and violent rotation of the stress direction in the crack development process, which is mainly affected by tensile stress. If the stress continues to rotate and the surrounding rock is sheared along the original crack plane, the protruding part is easy to separate and form fragments. Two shear cracks ④ and ⑤ develop at the position 1.0 m and 1.3 m away from the design profile of test tunnels, and their development directions are not much different from the original crack direction around them. From the spatial map, the crack plane of crack ④ is relatively straight, and it has an included angle of 45° with the borehole axis. However, the crack plane of crack ⑤ is affected by stress rotation during the development process, which leads to the development of concave-convex surface bending at a certain angle. The bending angle is basically the same as the stress rotation angle before the tunnel face advances to –10 m away from the monitoring section. The stress direction and fracture situation are shown in Fig. 17.

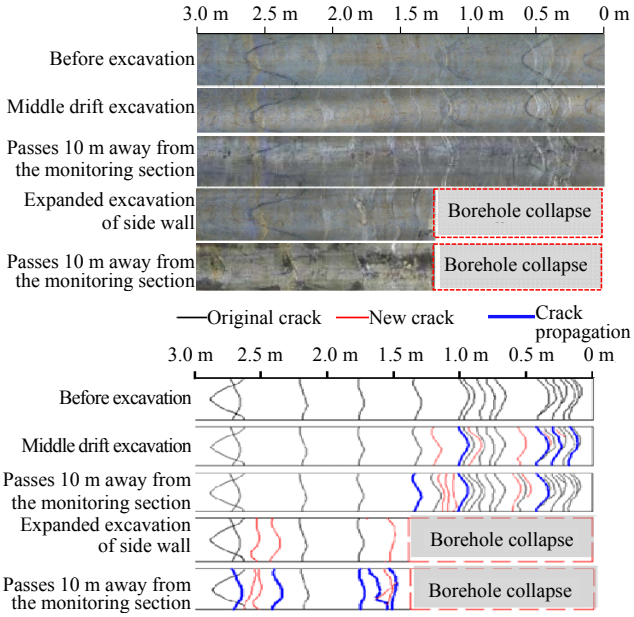

Fig. 16 Digital borehole image analysis about crack development

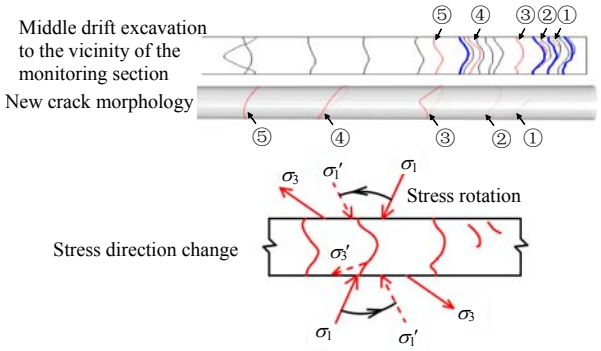

Fig. 17 Stress directions and crack development during middle pilot tunnel excavation (tunnel face moves towards monitoring section)

After the middle pilot tunnel is excavated for 10 m over the monitoring section, the principal stresses in three directions at the monitoring points slowly rotate nearly 20° in one month, the maximum rotation angle is less than 2° every day, and the maximum principal stress is along the direction perpendicular to the tunnel axis. The stress direction and fracture situation are shown in Fig.18. Two splitting tensile cracks ① and ②develop at the position nearly 0.5 m away from the design profile of test tunnels. The crack development direction is parallel to the original crack direction, and the crack development plane is deflected to a certain extent under the influence of stress rotation. Three shear cracks ③, ④ and ⑤ develop at the position

nearly 1.2 m away from the design profile of test tunnels. The crack planes all develop concave-convex surfaces bending a certain angle, and the bending angle is basically the same as the stress rotation angle. The crack develops in different periods during the small stress rotation process, resulting in a slight difference in the crack development direction.

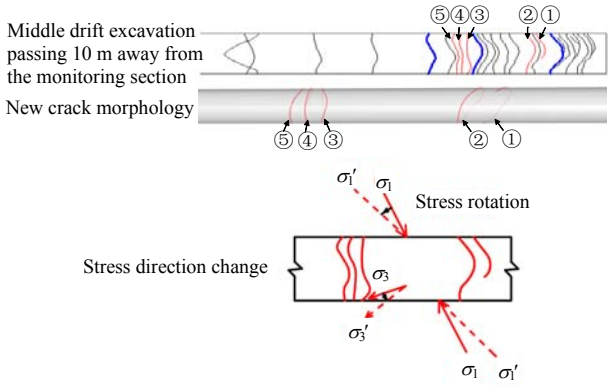

Fig. 18 Stress directions and crack development during middle pilot tunnel excavation (tunnel face moves away from monitoring section)

During the expanded excavation of side wall, the three principal stresses are adjusted in small ranges from 5° to 20° during the excavation from 10 m away from the monitoring section to 10 m over the monitoring section. Under the influence of stress rotation, a tensile-shear mixed crack ① with a slight deflection at the end develops at 1.6 m away from the design profile of test tunnels, and two shear cracks ② and ③ develop at nearly 2.5 m away from the design profile of test tunnels. Under the influence of stress rotation, the two shear cracks develop concave-convex surfaces bending at a certain angle, and the bending angle is basically the same as the stress rotation angle. The stress direction and fracture situation are shown in Fig. 19.

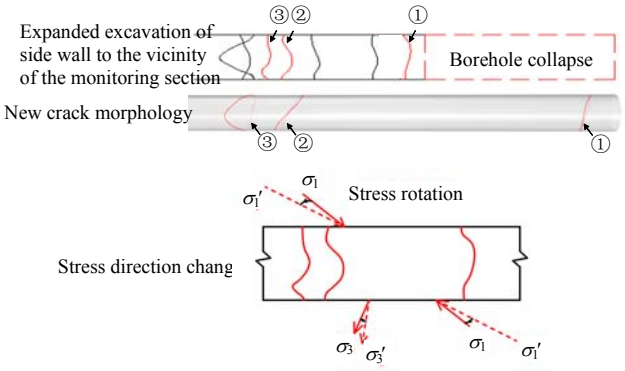

Fig. 19 Stress directions and crack development during expanded excavation of side wall (excavation face moves towards monitoring section)

During the expanded excavation of side wall, the stress state in the rock mass near the side wall is affected by the construction process after the excavation face passes 10 m through the monitoring section, and the local stress concentration leads to the failure of the broken rock mass near the free surface along the structural plane, resulting in spalling or collapse. In the borehole imaging, there are a lot of cracks in the rock mass within the length of 0-1.5 m, and the broken rock mass collapses along the direction of the crack surface at the position 1.5 m away from the design profile of test tunnel. After the borehole collapses, new cracks at the free surface form, and the stress in the rock mass is redistributed again with new crack production. From the imaging map, a series of new cracks begin to develop in the rock mass within the length of 1.5–3.0 m at this time. During this process, the three principal stress directions at the monitoring point rotate to a great extent (Fig. 10(c)), and the stress direction jumps back and forth twice with the maximum rotation angle approaching 90°. Under the action of stress rotation, two crossing X-shaped shear cracks ① and ②develop in the rock mass at nearly 1.6 m away from design profile of test tunnel, and the crossing angle of X-shaped cracks is basically the same as the stress rotation angle. At the same time, a tensile-shear mixed crack ③ with "protruding angle" develops at 1.6 m away from the design profile of test tunnel, and the crack direction deviates nearly 90° outward under the influence of stress rotation. A shear crack ④ develops at 2.5 m away from the design profile of test tunnel with a concave-convex surface bending at a certain angle of nearly 50°, as shown in Fig. 20.

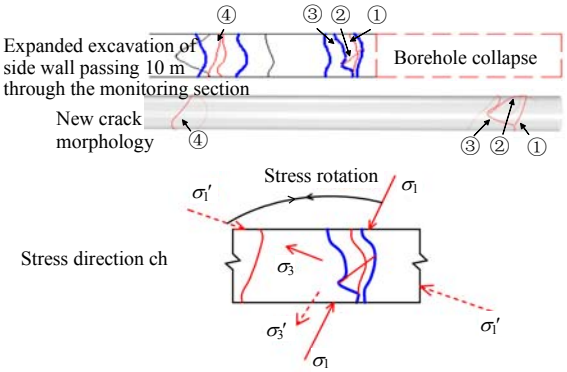

Fig. 20 Stress directions and crack development during expanded excavation of side wall (excavation face moves away from monitoring section)

4.3 Influence of stress rotation on rock fracture

According to the stress direction change and its corresponding rela0tionships with the formation and development of cracks, the fracture modes of surrounding rock disturbed by excavation are different under different change modes of stress direction.

(1) Tensile cracks and tensile-shear mixed cracks mostly develop in the rock mass near the free surface. This part of rock mass is highly disturbed by excavation and easily affected by unloading, and tensile cracks whose development direction changes

with the principal stress direction form within the rock mass, which is mainly affected by the rotation mode with large-angle stress mutation. The development direction of tensile cracks is affected by stress rotation, and the crack deviates from the original crack plane and develops along the direction of principal stress after rotation, forming secondary wing cracks that make the parallel cracks penetrate each other, thus reducing the rock mass stability. The crack morphology is characterized by the bifurcation of the original crack and the special crack morphology with "protruding angle". These two types of cracks are different from the parallel cracks around them, and they easily lead to the mutual penetration of the surrounding cracks, thus causing a series of tensile cracks, such as V-shaped spalling failure and wedge-shaped plate failure of rock mass.

(2) Shear cracks develop in the rock mass which is a little far from the free surface, and they are mainly affected by the stress direction change with small angle. The development of shear cracks affected by stress rotation will deflect at a certain angle, and shear cracks with concave-convex surface finally form with the deflection angle of crack surface equivalent to the stress rotation angle. This kind of cracks generally form under the large compressive stress, and have two forms of concave-outward and convex-outward shapes, which interlace with each other to form a shear dislocation zone similar to network.

(3) When the stress direction change is characterized as a large-angle gyration jump and the change reaches nearly 90°, two crossing X-shape shear cracks develop in rock mass under the action of this large-angle stress rotation, and the development of such cracks is easy to cause wedge-shaped shear failure in rock mass.

Under the action of stress rotation, the tensile-shear mixed crack with "protruding angle" and the shear crack with X-shaped crossing development make many cracks near them penetrate each other. At the same time, the change of principal stress direction not only promotes the formation of new cracks, but also leads to the further expansion of some original tensile and shear cracks, which easily causes the cracked rock mass to fall off and collapse outward.

5 Conclusions

Based on the real-time measured data of disturbed stress field in typical tunnels during excavation in Jinping Deep Underground Laboratory, the surrounding rock fracture induced by the disturbed stress field change during excavation in deep underground engineering was explored. The variation laws of disturbed stress angle at different spatial positions during middle pilot tunnel excavation and expanded excavation of side wall were analyzed, and the change mode of stress direction and its influence on the crack development in surrounding rock were summarized. The main conclusions are as follows:

(1) During middle pilot tunnel excavation and expanded excavation of side wall, the stress direction change in the surrounding rock mainly presents two modes of stress rotation and stress gyration. At the stage of middle pilot tunnel excavation, the stress change mode is mainly gyration when the tunnel face advances towards the monitoring section, while the stress change mode is mainly rotation when the tunnel face moves away from the monitoring section. During expanded excavation of side wall, the stress direction change mode at the monitoring point is mainly rotation when the excavation face advances, and the stress change mode appears as gyration only during new damage region development after side wall expansion.

(2) The stress change in surrounding rock caused by disturbance has an important influence on the morphology and strike of crack development. Under the action of stress rotation, the tensile cracks or tensile-shear mixed cracks is prone to develop in rock mass close to the free surface under the stress with large-angle rotation, and the cracks deviate from the original crack planes, resulting in secondary wing cracks that show the bifurcation of the original cracks and the special crack shape with "protruding angle". The curved shear cracks with concave-convex surfaces develop in rock mass far away from the free surface under the stress with small-angle rotation. However, under the action of large-angle stress gyration, crossing X-shaped shear cracks is prone to develop in rock mass, and they will aggravate the initiation and propagation of cracks no matter what stress change mode.

(3) The influence space of construction process on the direction of disturbed stress is limited, and the influence range is varying at different construction stages. The disturbed stress field changes the most actively at the stage of middle pilot tunnel excavation, the position where the principal stress direction change reaches the maximum is 4.5 meters away from the design profile of test tunnel. During the expanded excavation of side wall, the position where the change reaches the maximum is 2.5 meters away from the design profile of test tunnel, and the change occurs in the construction process after the excavation face is 10 m away from the monitoring section.

References

[1] MARTIN C D. The strength of massive Lac du Bonnet granite around underground openings[M]. Winnipeg: University of Manitoba, 1993.

[2] ZHENG Ying-ren, SHEN Zhu-jiang, GONG Xiao-nan. Principles of rock and soil plastic mechanics[M]. Beijing: China Building Industry Press, 2003.

[3] SHA Peng, WU Fa-quan, CHANG Jin-yuan. Unloading strength and failure pattern of marble under true triaxial test[J]. Chinese Journal of Rock Mechanics and Engineering, 2018, 37(9): 2084–2092.

[4] LIU Jie, ZHANG Li-ming, CONG Yu, et al. Research on the mechanical characteristics of granite failure process under true triaxial stress path[J]. Rock and Soil Mechanics, 2021, 42(8): 2069–2077.

[5] WANG Jia-chen, WANG Zhao-hui. Propagating mechanism of top-coal fracture in longwall top-coal caving mining[J]. Journal of China Coal Society, 2018, 43(9): 2376–2388.

[6] GAO Yao-hui, ZHNAG Chun-sheng, SU Fang-sheng, et al. Mechanism of stress-induced spalling of deep hard rocks under shear boundary condition[J]. Rock and Soil Mechanics, 2022, 43(4): 103–1111, 1122.

[7] PANG Yi-hui, WANG Guo-fa, LI Bing-bing. Stress path effect and instability process analysis of overlying strata in deep stopes[J]. Chinese Journal of Rock Mechanics and Engineering, 2020, 39(4): 682–694.

[8] ZHONG Li, CHEN Xin-lian, LIU Xiao-xuan, et al. Experimental study on the mechanical and deformation characteristics of calcareous sand under different stress paths[J]. Rock and Soil Mechanics, 2023, 44(10): 2929–2941.

[9] ZHANG She-rong, LIANG Li-hui. Analysis on tunnel liner supporting time considering three-dimensional stress rotation[J]. Journal of Hydraulic Engineering, 2007, 38(6): 704–709.

[10] SUN Chang-xin, HAN Li-xin, GAO Feng. Research on stress rotation and plastic deformation of cracks in tunnel during excavation[J]. Modern Tunnelling Technology, 2011, 48(1): 6–11.

[11] ZHANG C, ZHOU H, FENG X, et al. Layered fractures induced by principal stress axes rotation in hard rock during tunnelling[J]. Materials Research Innovations, 2011, 15(Suppl.1): 527–530.

[12] LI Jian-he, SHENG Qian, ZHU Ze-qi, et al. Analysis of stress path and failure mode of surrounding rock during Mine-by test tunnel excavation[J]. Chinese Journal of Rock Mechanics and Engineering, 2017, 36(4): 821–830.

[13] CHANG G F, HUA X Z, ZHANG J, et al. The mechanism of rock mass crack propagation of principal stress rotation in the process of tunnel excavation[J]. Shock and Vibration, 2021(11): 1–12.

[14] KAISER P K, YAZICI S, MALONEY S. Mining induced stress change and consequences of stress path on excavation stability: a case study[J]. International Journal of Rock Mechanics and Mining Sciences, 2001, 38(2): 167–180.

[15] EBERHARD T E. Numerical modelling of three-dimension stress rotation ahead of an advancing tunnel face[J]. International Journal of Rock Mechanics and Mining Sciences, 2001, 38(4): 499–518.

[16] DIEDERICHS M S, KAISER P K, EBERHARDT E. Damage initiation and propagation in hard rock during tunneling and the influence of near-face stress rotation[J]. International Journal of Rocks Mechanics and Mining Sciences, 2004, 41(5): 785−812.

[17] SHALEV E, LYAKGOVSKY V. The role of the intermediate principal stress on the direction of damage zone during hydraulic stimulation[J]. International Journal of Rock Mechanics and Mining Sciences, 2018, 107: 86–93.

[18] LI Shao-jun, ZHENG Min-zong, QIU Shi-li, et al. Characteristics of excavation disaster and long-term in-situ behavior of the tunnels in the China Jinping Underground Laboratory[J]. Journal of Tsinghua University (Science and Technology), 2021, 61(8): 842–852.

[19] ZHENG M Z, LI S J, ZHAO H B, et al. Probabilistic analysis of tunnel displacements based on correlative recognition of rock mass parameters[J]. Geoscience Frontiers, 2021, 12(4): 50–64.

[20] LI Shao-jun, XIE Zhen-kun, XIAO Ya-xun, et al. Review of international research on rock in situ rockmass behavior in deep underground research laboratory[J]. Journal of Central South University (Science and Technology), 2021, 52(8): 2491–2509.

[21] LI Shao-jun, ZHENG Min-zong. Development and engineering application of three-dimensional disturbed stress measurement system for deep hard rock engineering based on Fiber Bragg Grating[J]. Chinese Journal of Rock Mechanics and Engineering, 2023, https://doi.org/10.13722/j.cnki.jrme.2022.1182.

[22] ZHONG Shan, JIANG Quan, FENG Xia-ting, et al. A case of in-situ stress measurement in Chinese Jinping underground laboratory[J]. Rock and Soil Mechanics, 2018, 39(1): 356–366.

[23] LI Shi-yu, HE Tai-ming, YIN Xiang-chu. Rock fracture mechanics[M]. Beijing: Science Press, 2015.